Smoothed Particle Hydrodynamics for Numerical Solution of Filtration Problems

[1] Bashurov Vadim V., [2] Zhigalov Vladimir I.
[1]Research associate.
Lobachevsky Nizhny Novgorod State University. National studies
Nizhny Novgorod State University named after N.I. Lobachevsky,
bashurov@mail.ru, ORG ID 0000-0003-0754-1822
[2]Candidate of Physical and Mathematical Sciences, Doctor of Economics, title - senior researcher, position – chief researcher.
All-Russian Research Institute of Experimental Physics. Department
of Innovative Development, All-Russian Research Institute of Experimental Physics.
vlzhigalov@mail.ru , ORG ID 0000-0003-2898-3339

Article Info
Page Number: 836 – 848
Publication Issue:
Vol. 71 No. 3s2 (2022)

Article History
Article Received: 28 April 2022
Revised: 15 May 2022
Accepted: 20 June 2022
Publication: 21 July 2022

Abstract. The article is dedicated to the solution of the problems of water, gas and oil mixture filtration in homogeneous porous medium. The basic equations of the filtration theory are transformed into a special type for numerical approximation by the smoothed particle hydrodynamics. The numerical difference scheme is constructed based on the smoothed particle hydrodynamics. The algorithm of setting boundary conditions is proposed and isothermal one-dimensional and two-dimensional test numerical calculations of the process of water, gas and oil mixture filtration are given.

Keywords: modeling, computational optimization, smoothed particles, hydrodynamics, Darcy's equation.

Basic equations of the theory of mixture filtration in porous medium

The problem of numerical modeling of multicomponent medium dynamics based on [1] is considered. It is assumed that the continuous medium contains the system of pores, cracks and breaks whose typical dimensions are small in comparison with the physical size of the whole problem. The ratio between the pores volume and the total volume serves as the numerical characteristic of the medium porosity:

$$m = V_p/V$$

where m – porosity coefficient, V_p– pores volume, V – total volume of the given medium element. The multicomponent mixture flow through porous bodies is called filtration. Here, the part of the mixture having own physical and chemical properties and not changing its phase state during the modeling process is called the component one.

Pressure, temperature and saturation of each of the components are the main characteristics of the system motion. Saturation S_k of pore space of k component is the share of the pores volume occupied by this component in the elementary volume:

$$S_k = \frac{\Delta V_k}{\Delta V_p}, k = 1,2 \dots n$$

n – number of components in the mixture. The total of saturations of all components in the volume element equals 1:

$$\sum_{k=1}^{n} S_k = 1 \quad (1)$$

The minimum saturation exists for each component. These values are called "residual saturations" and are designated with index r. The simultaneous flow of phases is possible only in a certain interval of saturations. The notion of effective saturations of the components (are designated with the upper line symbol) is introduced for the work in this interval. The effective saturation of k component can be presented as follows:

$$\overline{S}_k = \frac{S_k - S_{kr}}{1 - \sum_{i=1}^{n} S_{ir}}$$

The main filtration law (Darcy's law) establishes the connection between the filtration velocity vector and pressure difference, which causes the filtration flow. The projection of filtration velocity u_k for each component in the space point along the arbitrary direction equals the ratio between the component volume rate and the side area perpendicular to this direction. It should be pointed out that Darcy's law plays the same role in the filtration theory as Fourier's law for the heat flow in thermal conductivity theory. Darcy's equation for k component, not taking into account the gravitation force, is written down as follows:

$$\mathbf{u}_k = -K\frac{c_k(S_n)}{\mu_k}\nabla P_k, \quad (2)$$

where K – characteristic of the porous medium called "absolute permeability", which does not depend on the mixture properties; μ_k – coefficient of the dynamic viscosity of k component $\mu_k = \mu_k(T)$); $c_k = c_k(S_n)$ – relative phase permeability of k component (can depend on the saturation of other components); P_k – pressure in k component. According to [2], there are limits to Darcy's law applicability.

Mass conservation law is another fundamental relationship in the filtration theory. The mass conservation law for each component is as follows:

$$\frac{\partial(m\rho_k S_k)}{\partial t} + \mathrm{div}(\rho_k \mathbf{u}_k) = 0, \quad (3)$$

here ρ_k – density of k component. By substituting (2) to expression (3), we obtain the basic equation of the filtration theory:

$$\frac{\partial(m\rho_k S_k)}{\partial t} = \nabla\left(\rho_k K\frac{c_k}{\mu_k}\nabla P_k\right) \quad (4)$$

The equation (4) will be further used for approximation with the help of smoothed particle hydrodynamics.

Equation of liquid and gas state

The problem of modeling the three-component mixture consisting of gas, water and oil, taking their compressibility into account, is set in the work. The following index notations for different components will be further used for convenience: w – water, n – naphtha (light oil), g – gas. The initial values of saturation, temperature and pressure are defined for each component. The densities are calculated by the corresponding equations of state for each component depending on the pressure and temperature. Water and oil components are considered as low-compressible and linearly dependent on the temperature and pressure difference:

$$\rho_k = \rho_{0k}(1 + \beta_k(P_k - P_0) + \alpha_k(T - T_0)), \quad (5)$$

where $k = w, n$ and ρ_{0k}– known density value of k component corresponding to the value of pressure P_0 and temperature T_0.

The equation of ideal gas state is assumed as true for the gas.

$$\rho_g = \rho_{0g}\frac{P}{P_0}\frac{T_0}{T} \quad (6)$$

Such physical and chemical parameters of the mixture as relative phase permeabilities and dynamic viscosities of the components are used during modeling. The relative phase permeabilities are found in accordance with Stone's approximation [2] and are presented in the analytical form. According to [2], the expression for the relative phase permeability of water is as follows: (нет выражения!)

where q=3.25. The relative phase permeabilities for oil and gas are similarly the analytical functions from the corresponding saturations. The dynamic viscosities for the mixture components are the analytical functions depending only on the temperature. According to [2], the dynamic viscosity of water is demonstrated by the following analytical expression:

$$\mu_w(T) = \frac{1}{29.21 \cdot T - 7506.64}.$$

The dependence of the relative phase permeability of water is given in Figure 1. The effective water saturation in the range from 0 to 1 is shown along the X-axis.

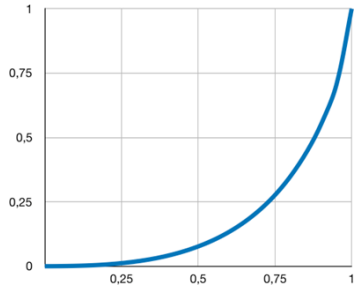

Fig. 1. Graph of the dependence of the relative phase permeability of water on the effective saturation

The graphic dependence of the water dynamic viscosity is given in Figure 2. The temperature measured in degrees K is shown along the X-axis. The dynamic viscosity is measured in Pa*sec.

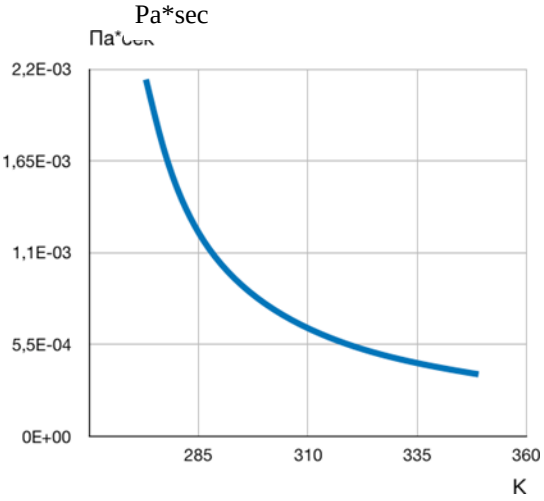

Fig. 2. Graph of the dependence of the water dynamic viscosity on the temperature.

Thus, the system of equations (4), (5), (6) is a closed one and is solved relative to the pressure, densities and saturations of the corresponding components.

Approximation of equations with smoothed particle hydrodynamics

Smoothed particle hydrodynamics (SPH) [3] is based on the smoothed integral interpolation of any scalar or vector magnitude defined in space. Smoothed interpolation $A_{SPH}(r)$ of some magnitude $A(r)$ is expressed in the form of integral:

$$A_{SPH}(r) = \int A(r')W(r - r', h)dr', \qquad (7)$$

where $W(r - r', h)$ - even function, also called "interpolation kernel", distributed around the space point r with typical size h. The integral from the smoothed function in the whole space equals 1.

$$\int W(r, h)dr = 1$$

When h tends to zero, function W(r,h) is converted into the delta-function. The graphic images of function W(r,h) (solid line) and its derivative W'(r, h) (dotted line) are demonstrated in Figure 3.

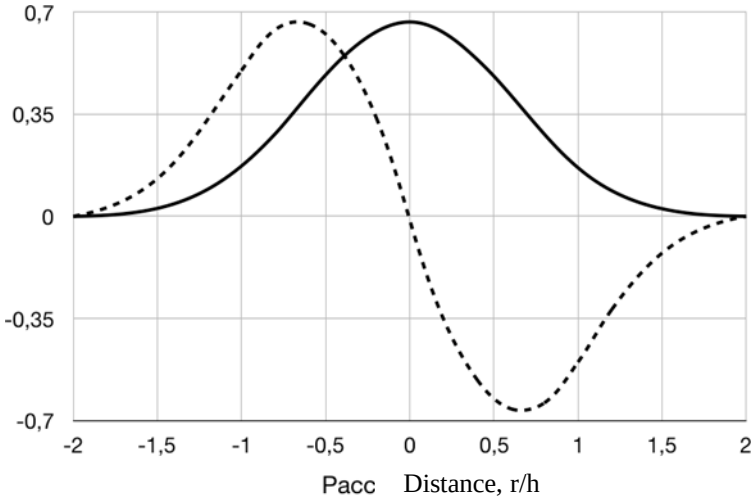

Fig. 3. View of smoothed function W and its derivative W'

The region, in which the problem is solved, is split into N elements with coordinates r_i, where i = 1,N. Each element is further called "a smoothed particle". Turning from the integration to summation in the expression (7) and replacing volume element dr′ by smoothed particle volume V_j, we obtain the basic formula for difference approximation of arbitrary function $A(r_i)$ in the defined space point r_i

$$A(r_i) = \sum_{j=1}^{N} V_j A(r_j) W(r_i - r_j, h) \tag{8}$$

Consequently, arbitrary function $A(r_i)$ by $_i$ is as follows:

$$\nabla A(r_i) = \sum_{j=1}^{N} V_j A(r_j) \nabla W(r_i - r_j, h). \tag{9}$$

The equations (8) and (9) are fundamental in the theory of smoothed particle hydrodynamics.

Historically, smoothed particle hydrodynamics (SPH) was proposed to solve astrophysical problems, for example, the universe divergence problem. Starting from 1990s, it has been widely used for modeling problems in hydrodynamics [4], in the solution of which high speeds and large deformations of continuous medium occur. At present, the researches on SPH application in different physical fields are being conducted. The algorithm of numerical solution of thermal conductivity problems with the help of smoothed particle hydrodynamics was proposed in [5], providing the basis for applying the difference algorithm of SPH in the filtration theory. This is connected with the fact that the differential equations of filtration and thermal conductivity have a similar mathematical form.

Smoothed particle hydrodynamics for Laplace equation

The first part of the equation (4) should be reconstituted for further approximation with smoothed particle hydrodynamics. Denoting $\phi = -K\frac{c}{\mu}$, the right part in the equation (4) is identically reconstituted.

$$\nabla(\phi\nabla A) = \frac{1}{2}(\nabla^2(\phi A) - A\nabla^2\phi + \phi\nabla^2 A). \quad (10)$$

The right part of the identity (10) contains the total of three Laplace differential operators, which should be numerically approximated by SPH. For the numerical approximation of Laplace operator, scalar magnitude A(r) is expanded in Taylor's series in neighboring space points r_i and r_j:

$$A(r_j) - A(r_i) = \nabla A(r_i)\cdot(r_j - r_i) + \frac{1}{2}\nabla^2 A(r_i)\cdot(r_j - r_i)^2 + \frac{1}{6}\nabla^3 A(r_i)(r_j - r_i)^3 + O(r_j - r_i)^4$$

Dropping the terms of order 4 and higher, both parts of the equation are multiplied by the expression:

$$\frac{(r_j - r_i)\cdot\nabla_j W(r_j - r_i, h)}{|r_j - r_i|^2}$$

Denoting further $r_{ij} = r_j - r_i$ and $W_{ij} = W(r_j - r_i h)$ and integrating by r_j, we obtain the integral representation for Laplace operator.

$$\nabla^2 A(r_i) = -2\int \frac{A(r_j) - A(r_i)}{|r_{ji}|^2} r_{ij}\nabla_j W_{ij} d^3 r_j$$

Turning from the integration to summation in the last formula and replacing volume element $d^3 r_j$ by smoothed particle volume V_j, we have the difference equation for the approximation of the integral representation of Laplace operator:

$$\nabla^2 A_i = -2\sum_{j=1}^{N} V_j \frac{A_j - A_i}{|r_{ji}|^2} r_{ij}\nabla_j W_{ij} \quad (11)$$

Laplace operators in the right part of the identity (10) are replaced by the expression (11). After uncomplicated arithmetical simplifications this identity is converted as follows:

$$\nabla(\phi_i\nabla A_i) = \sum_{j=1}^{N} V_j \frac{(\phi_i + \phi_j)(A_j - A_i)}{|r_{ji}|^2} r_{ij}\nabla_j W_{ij} \quad (11)$$

Consequently, the equation (4) acquires the final difference form

$$\frac{\partial(\rho_{ki}S_{ki})}{\partial t} = \frac{K}{m}\sum_{j=1}^{N} V_j \frac{(\rho_{ki}\frac{c_{ki}}{\mu_{ki}} + \rho_{kj}\frac{c_{kj}}{\mu_{kj}})(P_j - P_i)}{|r_{ji}|^2} r_{ij}\nabla_j W_{ij}, \quad (12)$$

Let us point out that the first derivative of smoothing function W_{ij} is used in the first part of the filtration difference equation (12).

The graph of derivative $W'(r,h)$, which is odd and equals zero beyond the interval $[-2,2]$, is shown with the dotted line in Figure 3 above. If smoothing function W is represented by the analytical expression

$$W(s,h) = \sigma_i\begin{cases} (2-s)^3 - 4(1-s)^3 & ,0 \le s < 1 \\ (2-s)^3 & ,1 \le s < 2, \\ 0 & ,2 \le s \end{cases}$$

where $s = r/h$ and $\sigma_1 = 1/(6h)$, $\sigma_2 = 15/(14\pi h^2)$and $\sigma_3 = 1/(4\pi h^3)$ for the cases of one-dimensional, two-dimensional and three-dimensional space, respectively, then its derivative is calculated by the formula:

$$W'(s) = \frac{3\sigma_i}{h}\begin{cases} (2-s)^2 - 4(1-s)^2 & ,0 \le s < 1 \\ (2-s)^2 & ,1 \le s < 2, \\ 0 & ,2 \le s \end{cases}$$

Time integration

The explicit difference scheme is used for the numerical calculation of thermodynamic parameters at the next time step. Denoting the right part of the expression (4) as F_{ki}, we get the following differential equation:

$$\frac{\partial(\rho_{ki}S_{ki})}{\partial t} = F_{ki} \quad (13)$$

The difference scheme of the first order of accuracy at the next time layer for the equation (13) is as follows:

$$P_{ki}^{n+1}S_{ki}^{n+1} = \rho_{ki}^{n}S_{ki}^{n} + \Delta t \cdot F_{ki} \quad (14)$$

where superscript n means the value of the corresponding magnitude at the time layer $t = t_n$. The integration step by time Δt is selected based on the condition of the difference scheme stability when solving Laplace equation $\Delta t = ch^2$, where $c<1$.

As a result, the system of seven equations (1), (5), (6), (14) is solved relative to the seven unknown quantities in each smoothed particle of space r_i

$P^{n+1}, \rho_k^{n+1}, S_k^{n+1}, k = [w, g, n]$.

When solving this problem of seven equations in each point r_j, new pressure, densities and saturations of the components at the next time layer $t = t_{n+1}$ are calculated. It can be easily seen that the system of seven equations (1), (5), (6), (14) is reduced to solving the cubic equation relative to pressure P^{n+1}.

Assuming the condition of water incompressibility $\rho_{wi}^{n+1} = \rho_{wi}^{n}$, the indicated system of equations (1), (5), (6), (14) is reduced to solving the quadratic equation relative to pressure P^{n+1}. Consequently, assuming the condition of water and oil incompressibility $\rho_{ki}^{n+1} = \rho_{ki}^{n}$, $k = w, n$, the system of equations (1), (5), (6), (14) is reduced to solving the linear equation relative to pressure P^{n+1}.

Boundary conditions

In the problems considered the boundary conditions of the first and second kind are used, which define the pressure on the computational region boundaries. The pressure can be defined by the explicit quantity $P = P_\Gamma$ or determined from the boundary flow condition $\frac{\partial P}{\partial n} = q_n$. Saturations can be defined by the explicit value on the region boundary $S_k = S_{k\Gamma}$, $k = w, n, g$.

To implement the boundary conditions, we use the algorithm of adding virtual particles, which are obtained with the help of the method of symmetric reflection of defined particles against the computational region boundary. Gas-dynamic parameters of the virtual particles are defined based on the boundary conditions.

Test calculations

The test calculations were carried out according to the described difference scheme.

The setting of the initial conditions for test problems was taken from [7]. In all problems the porosity, density and absolute permeability of the rock are considered constant in the whole volume, the residual saturations are assumed equal to zero, the region dimensions are 1 m × 1 m × 1 m.

The matrix consists of gas, water and naphtha. The naphtha density is less than the water density. The initial values of all dynamic parameters (saturation, temperature and pressure) are considered as defined for each component.

The medium is taken as isotropic in the whole volume considered, the liquid phases are assumed as low-compressible, the gas – ideal, the temperature and pressure are the same for all components of the mixture.

The temperature is considered constant during the whole modeling process. The gravitation is absent.

The following values for the parameters of the equations of state (5), (6) are used in the test calculations: $\rho_{0w} = 1000$ kg/m, $\rho_{0n} = 850$ kg/m, $\rho_{0g} = 1.4$ kg/m, $\beta_w = 4.4 \times 10^{-7}$ 1/Pa, $\beta_n = 10^{-6}$ 1/Pa, $\alpha_w = 1.32 \times 10^{-7}$ 1/K, $\alpha_n = 9.2 \times 10^{-7}$ 1/K.

The calculation results of one-dimensional test from [7] in graphical form are demonstrated in Figure 4. These calculations were made by the explicit difference scheme on the computational grid 50 nodes in size, regular and uniform by space.

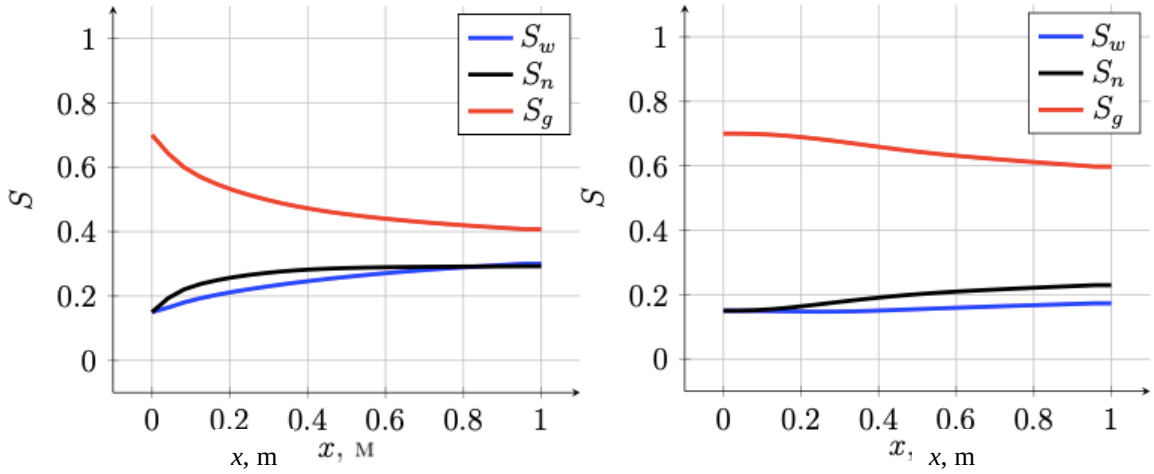

Fig. 4. Saturation profiles from [7] at the moments of time t = 5000 s (left graph) and t = 25000 s (right graph)

In this article, similar graphs of pressure and saturation distribution onto the corresponding time moments are formed based on the calculation results and the numerical modeling results are visually compared.

One-dimensional problem on gas injection under pressure

The one-dimensional model filtration problem is considered. The mixture flows due to the pressure difference at the ends of the considered interval in horizontal direction. The region size is 1 m. The gas is injected under pressure from the left to the right. The initial conditions: $S_w = 0.4, S_n = 0.3, S_g = 0.3, P_w = P_{atm}, T = 285K$. The boundary conditions for the saturations and pressure: $S_g|_{x=0} = 0.7, S_n|_{x=0} = 0{,}15\ S_w|_{x=0} = 0.15$, $P_w|_{x=0} = 1.1 * P_{atm}, P_w|_{x=1} = P_{atm}$. The rock parameters used: $K = 6.64 \cdot 10^{-11}$ m^2, m = 0.4. All values of the constants are given in SI system.

The step of integration by time Δt is selected due to the condition of difference scheme stability when solving Laplace equation $\Delta t = 0.25h^2$.

The typical time interval for calculating one problem is about 1-10 hours on a 2 GHz processor unit.

The calculation results with the number of particles N = 12 and typical size h = 0.15 m are given in Figures 5 and 6 in the form of profiles of components saturation and mixture distribution onto two time moments. The calculation results visually coincide with the results obtained when applying traditional regular grid methods taken from [7].

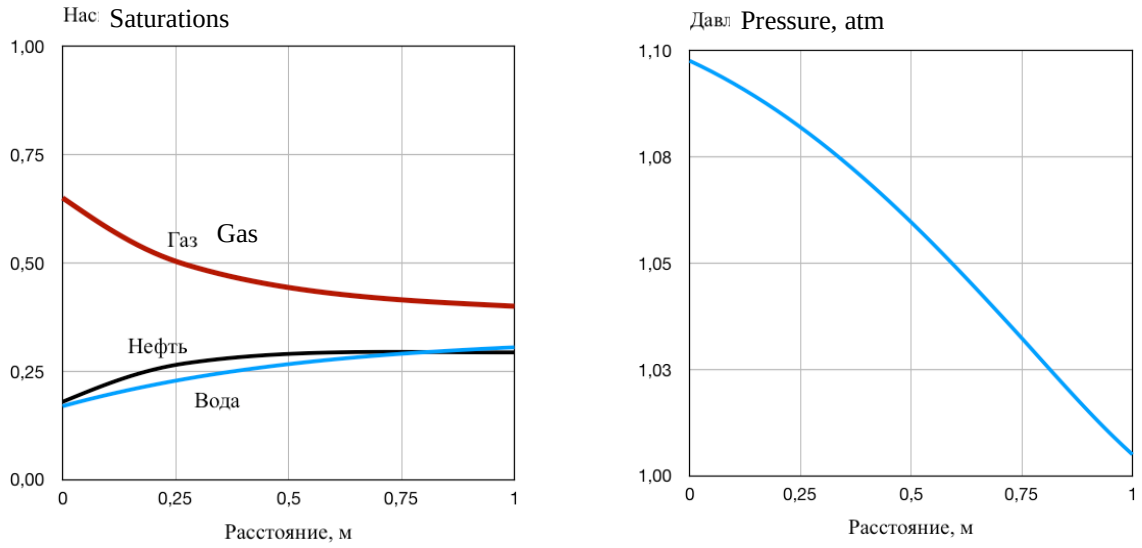

Fig. 5. One-dimensional test. Profiles of saturation (on the left) and pressure (on the right) at the moment of time t = 5000 s.

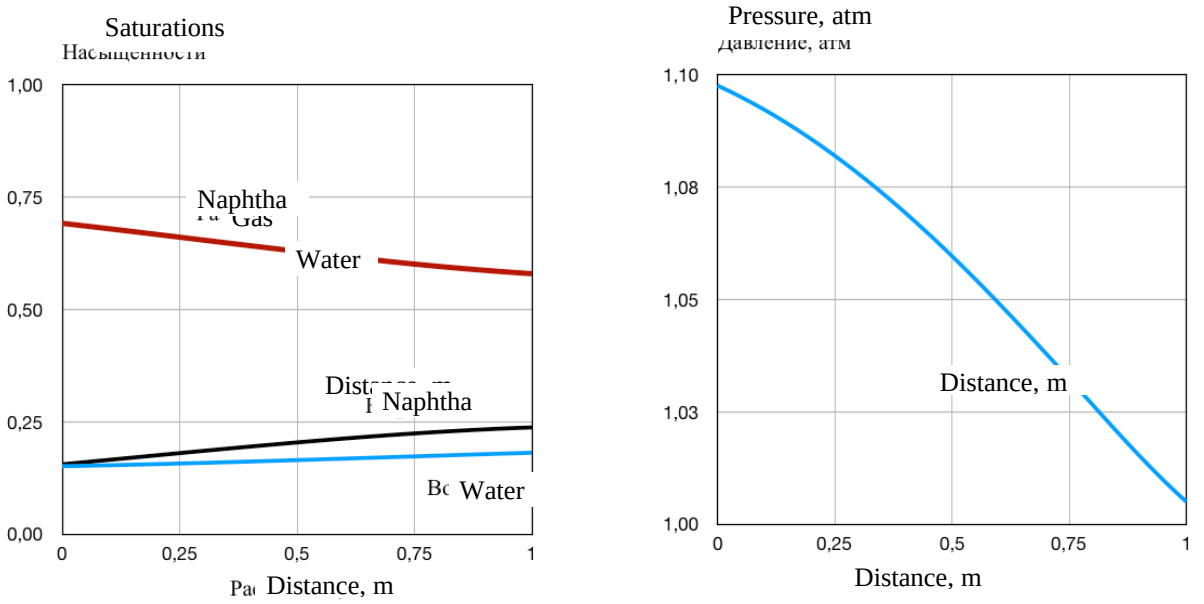

Fig. 6. One-dimensional test. Profiles of saturation (on the left) and pressure (on the right) at the moment of time t = 25000 s.

Two-dimensional test on gas injection under pressure

The physical and chemical parameters and initial conditions of the computational region for the two-dimensional test coincide with the values of the corresponding parameters from the one-dimensional problem. The region size is 1 m x 1 m. The gas is injected from the bottom left corner of the computational region. The boundary conditions for the saturations and pressure: $S_g|_{x=0\,\gamma=0} = 0.7, S_n|_{x=0\,\gamma=0} = 0.15$ $S_w|_{x=0\,\gamma=0} = 0.15$, $P_w|_{x=0\,\gamma=0} = 1.1 * P_{atm}, P_w|_{x=1\,\gamma=1} = P_{atm}$.

The number of smoothed particles varied during testing (from 10x10 up to 20x20). The typical time interval for calculating the problem was 20-100 hours. The calculation results for the two-dimensional test at the moment of time t = 5000 s are given in Figures 7 and 8. N = 11 x 11 particles were used in the calculations. The typical smoothing size was h = 0.15 m.

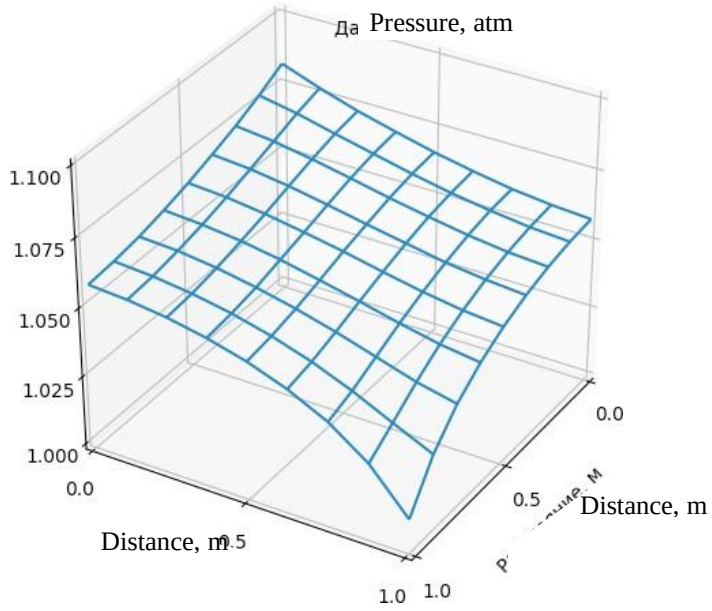

Fig. 7. Two-dimensional test. Pressure distribution at the moment of time t = 5000 s

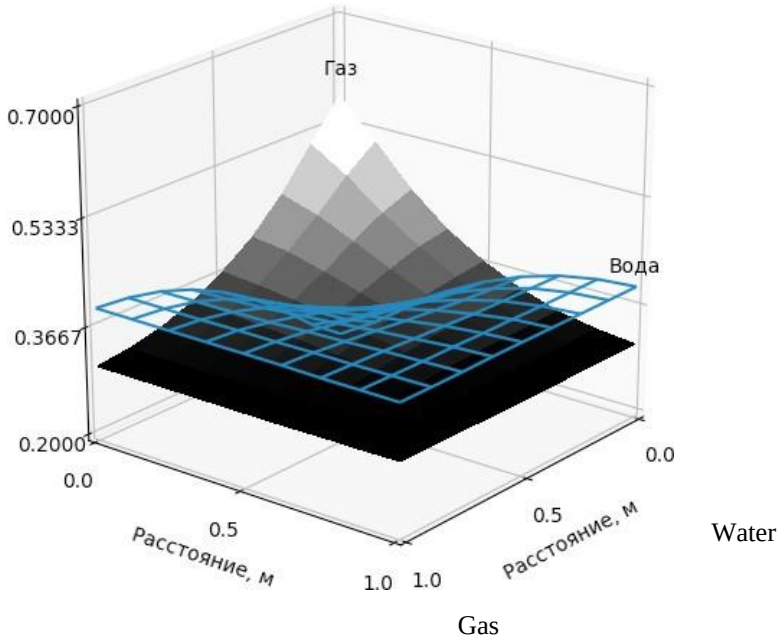

Fig. 8. Two-dimensional test. Distribution of saturations of water (mixture) and gas (solid surface) at the moment of time t = 5000 s.

Conclusion

In the process of numerical modeling of a real filtration process (for example, oil extraction from an underground deposit) it is important to construct a three-dimensional computational grid when the grid cell size in the drilling well region equals the typical size of the well mouth diameter of 15-30 centimeters, and the grid cell size at the boundary of the deposit region is 10-50 meters. This problem is solved by smoothed particle hydrodynamics. Besides, the smoothed particle hydrodynamics allows making the continuous computation of the physical processes both in the deposit and in the well.

In the result of the researches, the difference method of smoothed particle hydrodynamics to solve the filtration problem was developed and tested, and the prototype of the software system for modeling multidimensional filtration problems was created. The authors express their gratitude to Prof. S.P. Bautin for the discussion of the problem mathematical setting, precious advice and help in writing the article.

REFERENCES

1. Parker J.C., Lenhard R., Kuppusami T.A Parametric model for constitutive properties governing multiphase flow in porous media //Water Resources Research.-1987.-Vol. 23, no. 4.-p. 618–624.
2. Nouby M. Ghazaly, M. M. A. . (2022). A Review on Engine Fault Diagnosis through Vibration Analysis . International Journal on Recent Technologies in Mechanical and Electrical Engineering, 9(2), 01–06. https://doi.org/10.17762/ijrmee.v9i2.364
3. Aziz H., Settari E. Mathematical modeling of bedded systems.- Moscow: Nedra, 1982. -407p.
4. Gingold R.A., Monaghan J.J. Smoothed particle hydrodynamics: theory and application to non-spherical stars //Mon. Not. Roy. Astron. Soc.-1977. -375p.
5. Bashurov V.V., Bebenin G.V. etc. Experimental modelling and numerical simulation of high- and hypervelocity space debris impact to spacecraft shield protection //International Journal of Impact Engineering.-1997.-Vol. 20, Issues 1–5, 69-78p.
6. Jubelgas M., Springel V., Dolag K. Thermal conduction in cosmological SPH simulations //Mon. Not. Roy. Astron. Soc.-2004. -351p.
7. Owen J.M., Villumsen J.V., Shapiro P.R., Martel H. Adaptive Smoothed Particle Hydrodynamics: Methodology. II. The Astrophysical Journal Supplement Series, 1998. 155 209p.
8. Varun, B. N. ., S. . Vasavi, and S. . Basu. “Python Implementation of Intelligent System for Quality Control of Argo Floats Using Alpha Convex Hull”. International Journal on Recent and Innovation Trends in Computing and Communication, vol. 10, no. 5, May 2022, pp. 60-64, doi:10.17762/ijritcc.v10i5.5554.
9. Lyupa A.A., Trapeznikova M.A., Churbanova N.G. Modeling of non-isothermal multiphase filtration applying explicit difference schemes: Preprints № 103.- M:IAM, 2016.- 20 p.
10. Malla, S., M. J. . Meena, O. . Reddy. R, V. . Mahalakshmi, and A. . Balobaid. “A Study on Fish Classification Techniques Using Convolutional Neural Networks on Highly

Challenged Underwater Images". International Journal on Recent and Innovation Trends in Computing and Communication, vol. 10, no. 4, Apr. 2022, pp. 01-09, doi:10.17762/ijritcc.v10i4.5524.

11. Philip, A. M., and D. S. . Hemalatha. "Identifying Arrhythmias Based on ECG Classification Using Enhanced-PCA and Enhanced-SVM Methods". International Journal on Recent and Innovation Trends in Computing and Communication, vol. 10, no. 5, May 2022, pp. 01-12, doi:10.17762/ijritcc.v10i5.5542.
12. Pawan Kumar Tiwari, P. S. . (2022). Numerical Simulation of Optimized Placement of Distibuted Generators in Standard Radial Distribution System Using Improved Computations. International Journal on Recent Technologies in Mechanical and Electrical Engineering, 9(5), 10–17. https://doi.org/10.17762/ijrmee.v9i5.369
13. Rouzbahani F, Khoramshahi A A. Free convection flow and mass transfer over a vertical plate with radiation and uniform transpiration effects. sjfst. 2020; 2 (3) :11-24
URL: http://sjfst.srpub.org/article-6-63-fa.html